obtained at $\lambda=53°$N by several observers of star production[1-4] and neutron production.[2,5]

Furthermore, the latitude dependence[1] of star production under 312 g/cm^2 of air (30,000-feet pressure altitude) going from $\lambda=0°$ to $\lambda=55°$N shows the same characteristic increase of a factor of approximately 3.2 as already found for the neutrons[2] in the atmosphere, the exact factor depending upon the time of the measurements.

Thus, *both* the altitude and latitude dependence of the neutrons and stars in the atmosphere provide convincing evidence that the large atmospheric neutron production of initial energies below 10 to 20 Mev arises from the low energy nuclear disintegrations in the atmosphere. The change in absorption of the star producing radiation from approximately 150–160 g/cm^{-2} at $\lambda=53°$N to 210 g/cm^{-2} at $\lambda=0°$ is consistent with star production by nucleons where longer *nuclear collision chains* are formed from the higher energy primary particles at $\lambda=0°$.

Yuan[5] has determined the intensity of slow neutrons at $\lambda=53°$N with a maximum at approximately 9 cm Hg. It is of interest to extrapolate the star and neutron production[1,2] from equilibrium air pressures to the maxima of the curves at both $\lambda=0°$ and $\lambda=53°$N. Assuming the same general shape of maximum found by Yuan it would be expected that at $\lambda=0°$ the maximum would lie at a greater depth in the atmosphere because of the 210 g/cm^{-2} absorption. The extrapolated curves predict a factor of approximately 4 for the increase of neutron and star production at the maxima between 0° and 53°N.

At present, the approximate measurements of low energy star production in photo-emulsions near the top of the atmosphere between 30° and 53° by Schein, Lord, and Salant[6] are consistent with this extrapolation.

The writers particularly wish to thank Major Wayne Gustafson, Captains G. Freyer and Shawhan and the other officers and men of the U.S.A.F. B-29 at Inyokern, California for making these flights to Lima, Peru successful.

* Assisted by the Joint Program of the ONR and the AEC.
[1] J. A. Simpson, Jr. and R. B. Uretz, Phys. Rev. **76**, 569 (1949) and references therein.
[2] J. A. Simpson, Jr., Phys. Rev. **73**, 1389 (1948).
[3] Bridge, Hazen, Rossi, and Williams, Phys. Rev. **74**, 1083 (1948).
[4] Using the sensitive emulsion method: Bernardini, Cortini, and Manfredini, Phys. Rev. **76**, 1792 (1949), and references therein.
[5] L. C. L. Yuan, Phys. Rev. **74**, 504 (1948).
[6] Echo Lake Conference on Cosmic Rays, 1949.

Additional Electron Lines from Radioactive Europium*

J. M. Cork, H. B. Keller, W. C. Rutledge, and A. E. Stoddard
Department of Physics, University of Michigan, Ann Arbor, Michigan
February 6, 1950

PREVIOUS investigations[1] have shown many internally converted gamma-rays to be emitted by activated europium. The K–L–M differences observed for many of the electron lines are characteristic of gadolinium ($Z=64$) as would be expected for gamma-rays following beta-emission from europium ($Z=63$). For other lines, the K–L–M differences are characteristic of samarium ($Z=62$). This might have indicated an impurity in the original europium, but it is now quite certain that the samarium results from the K-capture process in europium 152, as an alternative mode of decay with beta-emission.

Table I. Electron energies from radioactive europium.

Electron energy kev	Interpretation	Energy sum $Z=62$ kev	Energy sum $Z=64$ kev	Electron energy kev	Interpretation	Energy sum $Z=62$ kev	Energy sum $Z=64$ kev
32.0	L(Auger)(62)	39.1		341.5	M^3(64)		343.4
37.9	M(Auger)(62)	39.1		361.9	$K(-)$	408.7 or	412.2
72.9	K^1(64)		123.2	398.2	K^4(64)		448.5
75.0	K^1(62)	121.8		439.9	L^4(64)		448.3
114.6	$L_{1,2}{}^1$(62)	122.1		471.7	$K(-)$	518.5 or	522.0
115.2	$L_{1,2}{}^1$(64)		123.4	536.7	$K(-)$	583.5 or	587.0
115.8	$L_3{}^1$(64)		123.1	561.5	$K(-)$	608.3 or	611.8
120.3	M^1(62)	122.0		608.5	$K(-)$	655.3 or	658.8
121.4	M^1(64)		123.3	640.3	$K(-)$	687.1 or	690.6
122.8	N^1(64)		123.2	673.6	K^3(62)	720.4	
197.6	K^2(62)	244.4		728.5	K^5(64)		778
236.4	L^2(62)	244.2		820.6	$K(-)$	868	871
242.4	M^2(62)	244.3					
286.0	K^2(64)		366.3	917	K^4(62)	964	
293.5	K^3(64)		343.8	954	L^4(62)	963	
328.5	L^2(64)		366.6	1039	K^5(62)	1086	
335.5	L^3(64)		343.6	1066	K^6(64)		1116

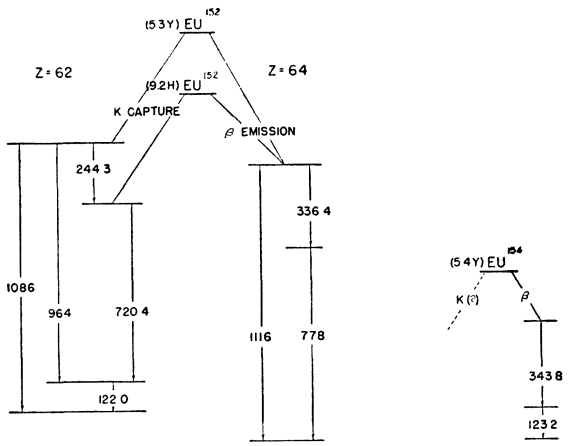

FIG. 1. Proposed europium decay schemes.

Inghram has shown by mass spectrometer studies that europium 152 and 154 have half-lives of 5.3 and 5.4 yr., respectively, and Muehlhause[2] has shown by critical absorption that K-capture occurred. Two of the gamma-rays observed (122 and 720 kev) are identical in energy with gamma-rays observed by Tyler in the 9.2-hr. europium activity due to K-capture.

In the present investigation with photographic magnetic spectrometers, the long-lived neutron activated europium yields in all about 33 electron lines as shown in column 1, Table I. Of these, about 26 lines may be uniquely identified as in samarium or gadolinium. The gamma-energies giving rise to them are summarized in Table II. For the remaining lines no K–L differences are observed and hence they are assumed to be K-lines for either samarium or gadolinium as shown in columns 3 and 4 of Table I, a choice to be made from further evidence.

By the use of a coincidence spectrometer (to be described elsewhere), Dr. C. M. Fowler has shown that electron-electron coincidences occur between the 122- and 244-kev gamma-rays and between the 123- and 344-kev gamma-rays, thus establishing certain sequences in emission, in agreement with the present interpretation.

Figure 1 indicates the complexity of the decay, and it presents that part of the existing information that seems reasonably certain and in agreement with the varied sources of information. For example, it can be seen how Tyler could observe from the 9.2-hr. activity certain, but not all, of the same gamma-energies observed here from the isomeric 5.3-yr. activity. The fit of the observed gamma-energies on the proposed level scheme is remarkably good.

Those gamma-rays due to transitions following beta-emission, and hence characteristic of gadolinium ($Z=64$), may occur in either Gd 152 or Gd 154. It is evident that a complete identifica-

Table II. Gamma-energies, identified.

Arbitrary number	$Z=62$ kev	$Z=64$ kev
1	122.0	123.2
2	244.3	336.4
3	720.4	343.8
4	964	448.4
5	1086	778
6		1116

tion of all electron lines can be made only when it is possible to obtain enriched isotopes of masses 151 and 153.

Since the sum of 336.4 and 778 kev is the observed 1115-kev line, this is arbitrarily shown as associated with Gd 152. The known sequence of 123- and 344-kev lines are shown together as arising from Gd 154. This will, of course, be much more complicated when the identification of all electron energies is complete.

* This investigation has been supported jointly by the AEC and ONR.
[1] A. W. Tyler, Phys. Rev. **66**, 125 (1939); M. G. Inghram and R. J. Hayden, Phys. Rev. **71**, 130 (1947); Cork, Schreffler, and Fowler, Phys. Rev. **72**, 1209 (1947); F. B. Shull, Phys. Rev. **74**, 917 (1948); and Hayden, Inghram, and Reynolds, Phys. Rev. **75**, 1500 (1949).
[2] C. Muehlhause, Manhattan Project Report CP-3750 (1947).

Cloud-Chamber Study of Cosmic Rays Underground*

O. L. TIFFANY AND W. E. HAZEN
Randall Laboratory of Physics, University of Michigan, Ann Arbor, Michigan
February 6, 1950

A COUNTER-CONTROLLED Wilson cloud chamber has been operated in a salt mine at a depth of 860 mwe (8.6×10^4 g/cm^2) from the top of the atmosphere. The primary aims of the experiment were two: First, to determine the character of the penetrating rays present at great depths and second, to investigate the properties of the secondaries that the penetrating rays produce in the salt roof above the cloud chamber and in lead, aluminum, and brass absorbers in the cloud chamber.

In order to determine whether or not the penetrating rays were ionizing, four one-inch lead plates were placed in the chamber with one tray of counters in the center of the chamber and the other tray below the chamber. A twofold coincidence between trays expanded the chamber and stereoscopic pictures were taken. With this arrangement, the pictures (aside from accidental coincidences) could be due to a single penetrating ionizing particle, to an electronic shower, or to a penetrating non-ionizing particle that produced two or more ionizing secondaries in the neighborhoods of the counters. Examination of the tracks in 175 pictures taken with this arrangement showed that 153 of the pictures were caused by single ionizing particles capable of traversing four inches of lead without unusual interactions. Eleven of the remaining pictures showed electronic showers, one of which was within the allowed region of the counter telescope, the remainder being side showers. Six accidentals were expected, leaving an upper limit of 5/153, or 3 percent, which might be caused by non-ionizing penetrating particles.

In order to investigate the electronic secondaries produced by the penetrating particles in the salt roof above the chamber, counter trays were placed above and in the center of the cloud chamber. The amount and nature of the absorber between the counters were then varied and the ratio of the number of soft particles with particular ranges to the number of penetrating particles was obtained. The results are summarized in Table I.

The penetrating particles were occasionally accompanied by secondary electrons upon emerging from the plates of lead, aluminum, or brass (center counter box). The ratios of accompanying secondary electrons to the producing penetrating particles are given in Table II. It is to be noted that these secondary electrons are more numerous than the knock-on electrons accompanying the penetrating component in lead at sea level. Nassar and Hazen[1] found about 6 percent for electrons of comparable energy range at sea level. The difference between the relative intensities of secondary electrons to penetrating particles in the mine and at sea level is most readily interpreted in terms of the expected difference in mean energies of the penetrating particles.

TABLE I. Absorption of electrons accompanying penetrating particles from salt roof.

Absorber	Penetrating particles	Electrons	Ratio electrons pen. part.
9 g/cm^2 Al+brass	108	75	70%
22 g/cm^2 Al+brass	100	16	16
66 g/cm^2 Pb (some Al+brass)	224	9	4

TABLE II. Secondary electrons produced in the chamber.

Absorber	Traversals	Electrons	Ratio-elec./p.p.
Pb	776 forward	162	
	808 backward	8	22 percent
Al	561	128	23
brass	420	73	17

If the penetrating particles traverse the entire layer of earth above the point of observation, we expect that a fraction $dI/I=2.9dh/h$ would be stopped in the absorber below the counters. Of a total of 454 penetrating particles, two were stopped while the expected number was about one. Thus it is unlikely that a significant number of the penetrating ionizing particles are produced in the earth.

Occasional large electron showers from the roof of the mine were detected in the chamber. Two very large showers were initiated in the chamber by single penetrating rays.

The pictures show that the majority of the penetrating particles at 860 mwe that are capable of producing twofold coincidences in a counter telescope are ionizing. These ionizing penetrating rays interact with matter in a manner that demonstrates qualitative resemblance with the penetrating rays at sea level. Since the average number of secondary electrons is higher and showers of electrons occur more frequently than at sea level, the average energy is apparently much higher.

We wish to express our appreciation for the assistance of the administration and personnel of the Detroit mine of the International Salt Company.

* This work has been assisted by the Joint Program of the ONR and the AEC.
[1] S. Nassar and W. E. Hazen, Phys. Rev. **69**, 298 (1946).

S-Matrix in Non-Local Field Theory

HIDEKI YUKAWA
*Columbia University, New York, New York**
January 26, 1950

RECENTLY the present author discussed certain types of quantized non-local fields, which were supposed to correspond to assemblies of elementary particles with finite radii.[1] In order to deal with the system consisting of two non-local fields, or a local field and a non-local field, which interact with each other, one must first find the substitute for the Schrödinger equation for the total system. However, it is naturally anticipated that the S-matrix in local field theory, which was obtained as the result of integration of the Schrödinger equation by successive approximations, may well find a counterpart in non-local field theory, whereas the physical interpretation of the Schrödinger wave functional itself, if it exists in non-local field theory, may be quite different from that in local field theory.

In fact, the S-matrix in non-local field theory can be obtained by a straightforward extension of the usual formalism. An arbitrary non-local operator A can be represented by a matrix $(n', x'|A|n'', x'')$, with rows and columns characterized by n', x' and n'', x'' respectively, where each of the symbols n', n'' stands for the distribution in numbers of particles in all possible quantum states while x' and x'' stand for a set of eigenvalues of four space-time operators x_μ. Further, we define $\{A\}$ for an arbitrary operator A by

$$(n'|\{A\}|n'')=\int\cdots\int(n', x'|A|n'', x'')(dx')^4(dx'')^4. \quad (1)$$

The S-matrix with matrix elements $(n'|S|n'')$ can now be written